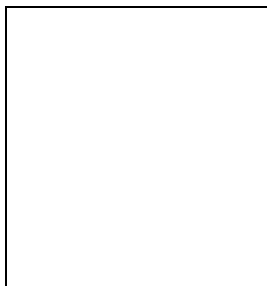


Phenomenological implication of KamLAND on lepton mass matrices

V. Antonelli, F. Caravaglios, R. Ferrari, M. Picariello

*Dipartimento di Fisica, Università di Milano via Celoria 16, I20133 Milano, Italy
and INFN, Sezione di Milano*



By using a model independent Monte Carlo approach, we study the possible structure of charged and neutral lepton mass matrices, under the assumption of an $U(2)$ horizontal symmetry (additional to the usual Standard Model ones) involving the light fermion generations. We assume the most general Majorana mass matrix for neutrinos. We update the results of our previous similar study, by inserting in the analysis the recent KamLAND data, that contributed to find a final solution to the Solar neutrino problem. The introduction of the new experimental data reduce the allowed regions in the nine dimensional parameter space, and show that our procedure gives stable solutions.

1 Introduction

Neutrino experimental physics has done big steps toward a full understanding of this interesting sector of elementary particle physics, also thanks to the recent data from Solar, atmospheric and reactor neutrino studies. These experiments have given a direct confirmation of the fact that the electron neutrinos produced in the Sun are converted into muon and tauon neutrinos before reaching the terrestrial detectors, in the same way as muon neutrinos produced by the cosmic rays are converted in something else during their fly in the atmosphere and in the Earth.

A simple and direct way to explain these observations is to assume that the mass eigenstates of the neutrinos differ from the eigenstates of the weak interaction (flavor eigenstates), as well as it happens in the quark sector. This gives rise to a new mixing matrix, similar to the CKM one, related to the lepton sector: the so called PMNS mixing matrix. From the theoretical point of view, there is still a lack of solid and unique interpretation of the entries of these mixing matrix.

The aim of this work is to give an indication of which class of theoretical models can explain better the experimental results in the lepton sector. We put ourselves in the quite general framework of non Abelian horizontal symmetries, whose advantages has been deeply discussed in literature¹. This means that we restrict our analysis to the models in which there is an additional $U(2)$ horizontal symmetry between the two lighter fermion generations, as explained

in². The consequence of this assumption is the fact that the charged lepton mass matrix has a particular structure, with some entries equal to zero. The class of matrices respecting this requirement is nevertheless quite general and inside this class we are looking for some typical textures characterizing the models which are in better agreement with the data.

The method used here for the updated neutrino data, including the recent results of KamLAND experiment, has been already applied to the study of the experimental implications in the quark sector³ and in the lepton sector² for the data before KamLAND⁴. Hence we refer the interested reader to these papers for a more detailed description of the adopted procedure. This method is based on the observation that all the theoretical models carry an intrinsic incertitude, because they are often completely unpredictable on the phases of the entries of the mixing matrix. It allows us to discriminate the models on the base of the fine tuning on the phases needed to explain the experimental data. The output of our analysis is an indication on which theoretical model needs a smaller fine tuning in the phases to be compatible with the experiments.

The work is organized as follows: in section 2 we discuss the experimental data from neutrino experiments and how we implement these experimental constraints; in section 3 we introduce a model independent neutrino mass matrix and then we explain the method used to fit the experimental data, we show our results and discuss how they can be used to discriminate between different theoretical models. The section 4 is devoted to the conclusions and outlook.

2 Neutrino physics

During the last seventy years big efforts have been done to understand neutrino physics. In particular a lot of experiments and theoretical discussions have created our knowledge about neutrino masses and lepton mixing angles. For a short review see for instance ref^{2,5,6} and references therein. In the first part of this section we analysis all the updated experimental data coming from different neutrino experiments. In the second part, instead, we discuss how we implement the experimental constraints in our analysis.

2.1 Experimental data from neutrino experiments

During the years many experiments investigated the problem of neutrino masses and they can be classified in different categories: the direct kinematical searches (observing mainly the tritium beta decay), the search for Neutrino-less Double β Decay ($N2\beta D$), and the experiments looking for signals of neutrino oscillation. In this last group of experiments different neutrino sources are used: atmospheric and Solar neutrinos and neutrino beams produced by accelerators or nuclear reactors and detected at a short distance (short baseline experiments) or very long distance (long baselines) from the production points.

The set of data we have considered for most of these different experiments are the same used in our previous analysis² (to which we refer the interested reader for a detailed discussion of these sets of data) or the corresponding updated data for the cases in which the experimental collaborations published a new data analysis during the last year.

The main exception is represented by the data concerning the mixing parameters determining the Solar neutrino oscillation. In fact very important results about these mixing parameters have been obtained in the last December by KamLAND collaboration^{7,8}. KamLAND⁹ is a reactor anti-neutrino experiment using anti-neutrino beams of the energy of a few MeV and with a baseline of about 200 Km. This experiment played an essential role in the final solution of the long standing Solar neutrino problem, because it is characterized by the right value of L/E in order to sound the so called LMA region, that is the region of the mixing parameters already selected by the Solar neutrino experiments ($\Delta m^2 \simeq 10^{-5} - 10^{-4} \text{ eV}^2$).

The first KamLAND results, even if characterized by a statistics that is still quite poor,

have been fundamental because they have given an independent confirmation of the neutrino oscillation hypothesis for mixing parameters in the typical region of Solar neutrinos and of the fact that the solution of the Solar neutrino problem is given by the Large Mixing Angle (LMA) solution. This solution is made possible by the interaction of Solar neutrinos with matter inside the Sun and the Earth (MSW effect) and is characterized by a mixing angle large, even if not maximal. A combined analysis of KamLAND data and of the evidences from all the Solar neutrino experiments⁸ gives two distinct sub-regions still compatible with the data inside the LMA solution. These regions are usually denoted as HighLMA and LowLMA, because they are characterized by different values of Δm^2 . As a matter of fact the LowLMA solution is by far the preferred one from a statistical point of view. Therefore in this analysis we are assuming this as the solution of the Solar neutrino problem, with the following values of the mixing parameters:

$$\log \left(\tan^2 \theta_{sol} \right) = -0.36 \pm 0.07. \quad \log \left(\frac{\Delta m_{sol}^2}{eV^2} \right) = -4.149 \pm 0.022.$$

We did not insert into our analysis the results found by the the LSND¹⁰ collaboration (signal of $\bar{\nu}_\mu \rightarrow \bar{\nu}_e$ oscillation with high value of δm^2), whose explanation would require to introduce a sterile neutrino in addition to the usual three generations of the Standard Model or more exotic theories.

2.2 Implementation of the experimental constraints

In our analysis we introduced all the experimental constraints on neutrino physics that we have discussed in the previous section, with the exception of the LSND results. We implemented the constraints on the mass differences by assuming Gaussian errors in logarithmic scale for Δm_{atm}^2 , $\sin^2 2\theta_{atm}$, Δm_{sol}^2 and $\tan^2 \theta_{sol}$, where the self explanatory notation refers to the variables defined in the previous subsection and in our previous analysis². This approximation, based on the fact that our knowledge of the neutrino physics parameters is limited only to the order of magnitude, introduces a second order indetermination that can be neglected for our purposes. To apply the experimental constraints we defined the following set of observables

$$\mathcal{O}_i \in \left\{ \log \Delta m_{atm}^2, \log \sin^2 2\theta_{atm}, \log \Delta m_{sol}^2, \log \tan^2 \theta_{sol}, < m_\nu > \right\} \quad (1)$$

and we introduced the χ^2 function of the configuration \mathcal{R} of the neutrino mass matrix:

$$\chi^2(\mathcal{R}) = \sum_i \left(\frac{\mathcal{O}_i^{th}(\mathcal{R}) - \mathcal{O}_i^{exp}}{\sigma_i^{exp}} \right)^2. \quad (2)$$

In the previous equation, $\mathcal{O}_i^{th}(\mathcal{R})$ is the value of the i^{th} observable calculated for the configuration \mathcal{R} , and \mathcal{O}_i^{exp} and σ_i^{exp} are respectively the experimental value and its error for the same observable. We also introduced the upper limits for the neutrino masses coming from the direct kinematical searches, but these limits modify in a negligible way our results and we could completely neglect them.

3 Lepton mass matrices

The Standard Model (SM) has a very high predictive power which has been tested in the high precision measurements of particle physics. It allows us to obtain quarks, leptons and bosons masses by using the Higgs mechanism and by introducing a set of coupling constants, which are also related to the particle masses and the so called mixing angles. While this mechanism is implemented in a natural way and experimentally confirmed with very high precision, the

coupling constants, and then the particle masses and the mixing angles, introduced cannot be theoretically determined inside the SM. An explanation can come by assuming that the SM is a low energy effective theory of a more fundamental one, where the full Lagrangian contains other fields and the coupling constants are simpler. In this scenario only the light fields appear in the low energy spectrum, while heavy fields decouple. Due to the freedom in taking the full Lagrangian, one can obtain models which give the rich spectrum of the SM at low energy. However symmetries, simplicity and naturalness induce us to decide for a model instead of an other. A criteria for naturalness is assumed to be how much one has to fine tune the parameters introduced in the full Lagrangian to reproduce the SM, and our analysis is basically founded on this idea. To emphasize that, we first introduce a model independent parameterization of the Lagrangian of the leptons sector and than we discuss the method we used to fit the experimental data within our parameterization.

3.1 A model independent parameterization

In our analysis we did not introduce any light particles additional to the ones usually introduced in the SM. In particular we did not introduce any right partner of the neutrinos. However we introduce an effective Majorana term for the left handed neutrinos. The low energy kinetic terms in the Lagrangian of the leptons can be characterized, after the $SU(2) \times U(1)$ spontaneous symmetry breaking, with a matrix M that gives the masses of the charged leptons and a matrix m giving the neutrino masses. The two matrices give rise to the so called mixing angles. In particular, the eigenvalues of M are very well determined by the experiments on the charged lepton masses, while m and the mixing angles are determined by the neutrino experiments discusses in section 2. Following the hint given by the theoretical models we parameterize M and m by introducing an exponential parameterization of the entries of the matrices:

$$m = m_0 \begin{pmatrix} a_{11}\lambda^{v_{11}} & a_{12}\lambda^{v_{12}} & a_{13}\lambda^{v_{13}} \\ a_{21}\lambda^{v_{21}} & a_{22}\lambda^{v_{22}} & a_{23}\lambda^{v_{23}} \\ a_{31}\lambda^{v_{31}} & a_{32}\lambda^{v_{32}} & a_{33}\lambda^{v_{33}} \end{pmatrix} \quad M = m_l \begin{pmatrix} 0 & b_{12}\varepsilon_1^{1-p} & 0 \\ b_{21}\varepsilon_1^p & \varepsilon_2 & b_{23}\varepsilon_2^r \\ 0 & b_{32}\varepsilon_2^d & b_{33} \end{pmatrix} \quad (3)$$

where we put for convenience $m_0 = 0.06 \text{ eV}$, $m_l = m_\tau$ and $\lambda = 0.2$. The exponents v_{ij} are real number which give rise to the order of magnitude of the entry i, j . The coefficients a_{ij} and b_{ij} are complex number of module one and allow us to introduce generic phase for each entry. We remember that the matrix m is symmetric due to the Majorana nature of the quadratic neutrino terms, i.e. we must taken $a_{ij} = a_{ji}$ and $v_{ij} = v_{ji}$.

3.2 Fitting the experimental data: the method

The goal of this work is to extract the values of the exponents v_{ij} from the experimental measurements. A direct fit of the data is not possible, since the number of free parameters in eq. (3) is much larger than the number of observables, three mass eigenvalues plus the mixing angle parameters. The main obstacle comes from the coefficients a_{ij} whose phases are often theoretically unpredicted and are assumed to be any number in the range $0 - 2\pi$ while sometimes they are constraints up to 1-10%. We treat this uncertainty as a theoretical systematic error. Namely, we have assigned a flat probability to all the coefficients a_{ij} with

$$0 < \arg(a_{ij}) < 2\pi, \quad |a_{ij}| = 1. \quad (4)$$

For the theoretical models that unpredicted these phases, our analysis apply in a straightforward way. A model will be more competitive than another, in the sense that it needs a smaller fine tuning in the phases a_{ij} , if the ball in the parameter space corresponding to this models falls

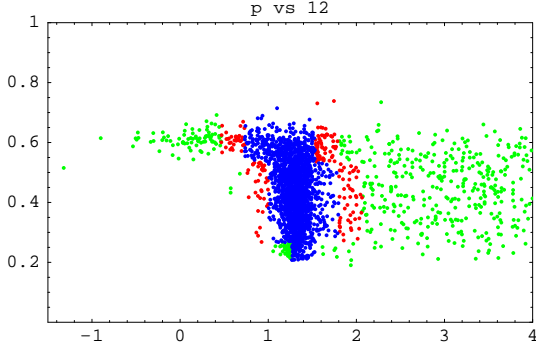


Figure 1: The exponent p versus the exponent v_{12} .

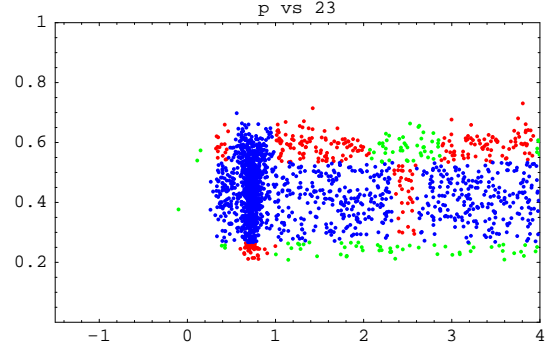


Figure 2: The exponent p versus the exponent v_{23} .

in a higher density region. In the other case a more careful discussion is needed but important informations on the fine tuning of the phases can be obtained from our results.

The exponents v can take any value: in practice we have chosen an interval $-2 < v_{ij} < 4$. We choose these limits because for a value of v bigger than 4 the relative entry is so close to zero that it is negligible; we have checked that no v is smaller than -2 even if we enlarge the allowed interval. For any random choice of the coefficients a_{ij} and the exponents v_{ij} we get a numerical matrix for the neutrino sectors. The diagonalization of this matrix gives us three eigenvalues, corresponding to the predicted physical neutrino masses, and a numerical unitary matrix which correspond to the MNS mixing matrix. We have collected a large statistical sample of events. Each one of these events can be compared with the experimental data through a Monte Carlo by using the χ^2 analysis explained in section 2.2. An event is accepted with probability given by the exponential weight χ^2 defined in eq. (2).

Even if our Monte Carlo approach favors most predictive and accurate models, we also emphasize that one should not mistake these results with true experimental measurements. They only give us natural range of values for the exponents v .

3.3 The results

We report in figures the correlation between the i entries for neutral mass matrix with the p -entry for the charged lepton mass matrix, and the correlation between the p , r and d entries for the charged lepton mass matrix. We show eight figures corresponding to different pairings of the exponents. By looking at the six figure containing the neutral mass matrix entries, it is evident that there is a symmetry: the one under the swapping of the 2^{nd} and 3^{rd} neutrino. This symmetry is evident by looking at the symmetry under exchange of fig. 1 and fig. 3, and

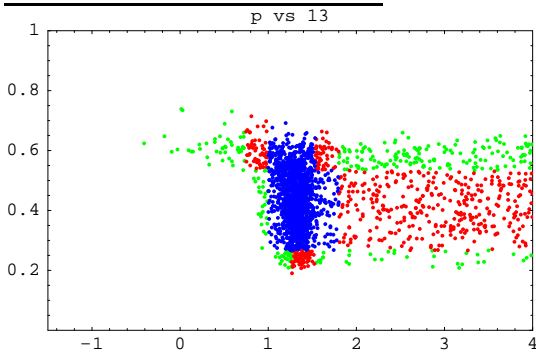


Figure 3: The exponent p versus the exponent v_{13} .

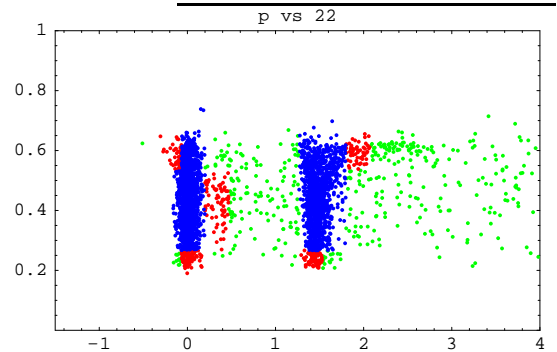


Figure 4: The exponent p versus the exponent v_{22} .

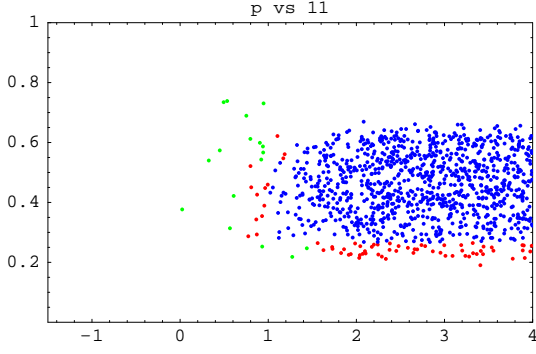


Figure 5: The exponent p versus the exponent v_{11} .

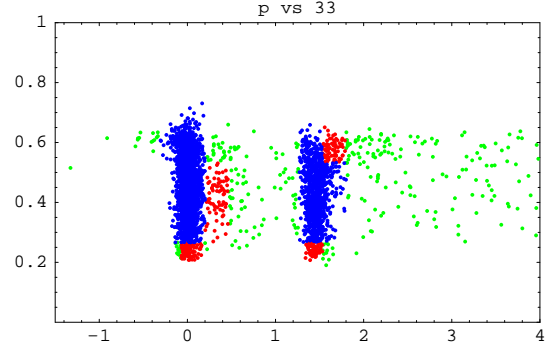


Figure 6: The exponent p versus the exponent v_{33} .

the equivalence between fig. 4 and fig. 6. From figs. 1-3-6 we see that there is the possibility to have the three entries 12-13-33 very near and in the range $0.06 \leftrightarrow 0.1$ eV. A deeper investigation of the data set gives that the other neutrino mass matrix entries are one order of magnitude smaller. Moreover the same figures show that the exponent p is about 0.6. We notice that this is consistent with the maximal atmospheric mixing angle and the large Solar mixing angle, due to the high mass degeneracy. From figures we find the the exponent p is constrained to be between 0.2 and 0.6. From fig. 1 and fig. 3 we find that the entries 12 and 13 have to be bigger then one except the degenerate case considered before, and the case $v_{12}(v_{13}) \approx 1.2 \pm 0.2$ is preferred. Fig. 2 tells us that the entry 23 is bigger than 0.2 and $v_{23} \approx 0.6 \pm 0.3$ is statistically enhanced. Form figs. 4-6 we conclude that the exponents v_{22} and v_{33} are bigger than -0.4 and the values 0 ± 0.3 and 1.5 ± 0.3 are the preferred ones. Finally, form fig. 5 we obtain that the exponent v_{11} is bigger than zero (except in the particular case of *high* mass degererances).

4 Conclusions and outlook

Our results show a symmetry under the swap of 2^{nd} and 3^{rd} neutrinos: one can interchange the entry 22 with the 33, and the entry 12 with the 13. We find that there are two kinds of texture which are more compatible with the atmospheric, Solar, reactor and kinematic experiments:

- The case where

$$v_{11} > 1; \quad v_{12} > 1; \quad v_{13} > 1; \quad v_{22} > -0.3; \quad v_{23} > 0.3; \quad v_{33} > -0.3; \\ 0.2 < p < 0.6; \quad d > 0; \quad r < 0.5.$$

This non-degenerate case have the entries 22, 23 and 33 of order 0.06 eV (to explain the large mixing angle and the Δm_{atm}^2), while the other entries have to be at least one order of magnitude smaller (to explain the Δm_{sol}^2).

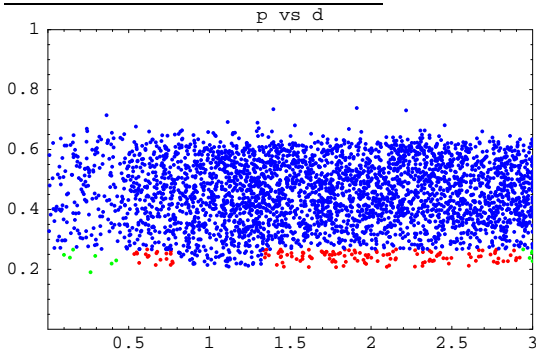


Figure 7: The exponent p versus the exponent d .

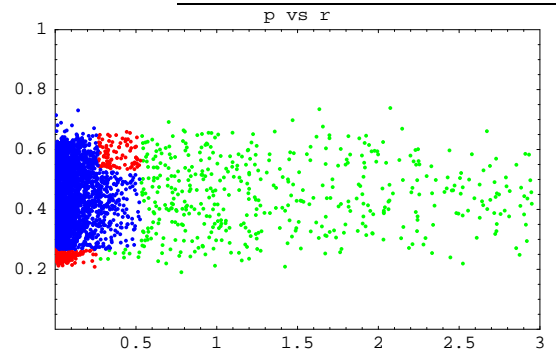


Figure 8: The exponent p versus the exponent r .

- The quasi-degenerate case, in which the neutrino masses are bigger than 0.06 eV (but smaller than 0.7 eV). This degenerate case can be reached in tree ways: one diagonal entry and the off-diagonal entry of the residual 2 by 2 matrix block between 0.06 and 0.7 eV , and all the other entries smaller.

In our results there is a hint for an asymmetric non trivial texture in the charged lepton sector. Combined with an analogous result in the down quark mass matrix³, this can be interpreted as a new hint of $SU(5)$ grand unification².

Acknowledgments

We are deeply grateful to E. Torrente-Lujan and to P. Aliani for many useful discussions about neutrino physics. We acknowledge the financial support of the Italian MIUR. The numerical computations have been performed in the computer farm of the Milano University theoretical group.

References

1. R. Barbieri, L. J. Hall and A. Romanino, Nucl. Phys. **B551** (1999) 93 and references therein; R. Barbieri, G. R. Dvali and L. J. Hall, Phys. Lett. B **377** (1996) 76; Z. G. Berezhiani, Phys. Lett. B **150** (1985) 177; P. Pouliot, N. Seiberg, Phys. Lett. B **318**, 169 (1993); A. Pomarol and D. Tommasini, Nucl. Phys. B **466** (1996) 3
2. V. Antonelli, F. Caravaglios, R. Ferrari, M. Picariello Phys.Lett. B 549 (2002) 325-336
3. F. Caravaglios, P. Roudeau and A. Stocchi, Nucl. Phys. B **633** (2002) 193
4. J. N. Bahcall, M. C. Gonzalez-Garcia and C. Pena-Garay, JHEP **0207** (2002) 054
S. Pascoli and S. T. Petcov, Phys. Lett. B **544** (2002) 239
P. Aliani *et al.*, Phys. Rev. D **67** (2003) 013006
P. Aliani, V. Antonelli, M. Picariello and E. Torrente-Lujan, New J.Phys. **5** (2003) 2
P. Aliani, V. Antonelli, M. Picariello and E. Torrente-Lujan, Nucl. Phys. B **634** (2002) 393
V. Barger, D. Marfatia, K. Whisnant and B. P. Wood, Phys. Lett. B **537** (2002) 179
A. Bandyopadhyay, S. Choubey, S. Goswami and D. P. Roy, Phys. Lett. B **540** (2002) 14
R. Foot and R. R. Volkas, Phys. Lett. B **543** (2002) 38
P. C. de Holanda and A. Y. Smirnov, arXiv:hep-ph/0205241;
A. Strumia, C. Cattadori, N. Ferrari and F. Vissani, Phys. Lett. B **541** (2002) 327.
5. S. M. Bilenky, arXiv:hep-ph/0205047; P. Aliani *et al.*, arXiv:hep-ph/0206308.
6. G. Altarelli and F. Feruglio, arXiv:hep-ph/0206077; A. Strumia and F. Vissani, Int. J. Mod. Phys. A **17** (2002) 1755.
7. K. Eguchi *et al.*, [KamLAND Collaboration], Phys. Rev. Lett. **90** (2003) 021802
F. Suekane [KamLAND Collaboration], Nucl. Phys. Proc. Suppl. **111** (2002) 128.
8. G. Fiorentini *et al.*, Phys. Lett. B **558** (2003) 15
P. C. de Holanda and A. Y. Smirnov, JCAP **0302** (2003) 001
G. L. Fogli *et al.*, arXiv:hep-ph/0212127.
P. Aliani, V. Antonelli, M. Picariello and E. Torrente-Lujan, arXiv:hep-ph/0212212.
J. N. Bahcall, M. C. Gonzalez-Garcia and C. Pena-Garay, JHEP **0302** (2003) 009
A. Bandyopadhyay *et al.*, Phys. Lett. B **559** (2003) 121
V. Barger and D. Marfatia, Phys. Lett. B **555** (2003) 144
9. H. Murayama and A. Pierce, Phys. Rev. D **65** (2002) 013012
B. C. Chauhan, J. Pulido and E. Torrente-Lujan, arXiv:hep-ph/0304297
E. Torrente-Lujan, arXiv:hep-ph/0302082.
P. Aliani, V. Antonelli, M. Picariello and E. Torrente-Lujan, JHEP **0302** (2003) 025
10. M. Sung, Int. J. Mod. Phys. A **16S1B**, 752 (2001)